

Bayes DistNet - A Robust Neural Network for Algorithm Runtime Distribution Predictions

Jake Tuero, Michael Buro

Department of Computing Science, University of Alberta
Edmonton, Canada
{tuero, mburo}@ualberta.ca

Abstract

Randomized algorithms are used in many state-of-the-art solvers for constraint satisfaction problems (CSP) and Boolean satisfiability (SAT) problems. For many of these problems, there is no single solver which will dominate others. Having access to the underlying runtime distributions (RTD) of these solvers can allow for better use of algorithm selection, algorithm portfolios, and restart strategies. Previous state-of-the-art methods directly try to predict a fixed parametric distribution that the input instance follows. In this paper, we extend RTD prediction models into the Bayesian setting for the first time. This new model achieves robust predictive performance in the low observation setting, as well as handling censored observations. This technique also allows for richer representations which cannot be achieved by the classical models which restrict their output representations. Our model outperforms the previous state-of-the-art model in settings in which data is scarce, and can make use of censored data such as lower bound time estimates, where that type of data would otherwise be discarded. It can also quantify its uncertainty in its predictions, allowing for algorithm portfolio models to make better informed decisions about which algorithm to run on a particular instance.

1 Introduction

Many of the algorithmic solvers for NP-complete problems, such as CSP and SAT, rely on backtrack methods. These solvers can have runtimes which vary substantially, depending on whether they make mistakes caused by sub-optimal heuristics during the recursive backtrack calls. Adding randomization and restarts into the backtrack algorithms has been shown to help alleviate some of the heavy-tail nature that these runtimes exhibit, decreasing the algorithm’s runtime by many orders of magnitude in some cases (Harvey 1995; Gomes, Selman, and Kautz 1998).

If the underlying *runtime distribution* (RTD) is known for a particular algorithm, then an optimal fixed cutoff-time restart strategy can be formulated (Luby, Sinclair, and Zuckerman 1993). Knowing the underlying RTD can also lead to efficient use of algorithm portfolios, which can dynamically assign algorithms to input instances based on the predictive RTD. These are just a few reasons why it’s important to have

models which are robust and can give accurate RTD predictions for unseen instances.

The current state-of-the-art RTD prediction models are designed to give exact parametric distributions as output, with the model predicting the particular distribution parameters (Eggenesperger, Lindauer, and Hutter 2018). However, these models make the assumption that the particular algorithms on the given instances follow a particular parametric distribution. These models also tend to have their predictive power hindered in the presence of a small number of observations per input instance or with censored examples (only a lower bound for the runtime is known). The goal of our research is to have a robust model under these conditions, and to try to lift some of the restrictions we put on the models.

The rest of this paper is organized as follows. We first give a summary of the two areas our research joins for the first time: randomized algorithm runtime prediction and Bayesian deep learning. We then show how our model extends existing methods into the Bayesian setting, and show how effective our model is in several scenarios. Finally, we give some insights into where we think the next research steps are for extending our work.

2 Background and Related Work

In this section, we give an overview of randomized algorithm runtime prediction and Bayesian learning in neural networks.

Randomized Algorithm Runtime Prediction

Problems such as CSP and SAT are NP-complete, meaning that there is currently no guarantee there is a polynomial time solution technique. The dominant solver technique for these types of problems is backtrack search, in which heuristics pick an unbound variable, assign a value to it, and the search proceeds recursively. If an inconsistency is detected, the algorithm backtracks and tries another assignment to that variable.

A consequence of using backtrack-based solvers is that early mistakes can cause long searches down branches of the search tree which eventually need to be backtracked. This leads to the so-called “heavy-tail” phenomenon, in which the runtime of these algorithms exhibit tails which are not exponentially bounded. Harvey (1995) was the first to show that adding randomization and restarts into the backtracking

algorithm can alleviate the issue of wasting time on eventual dead-ends. Gomes, Selman, and Kautz (1998) presented general methods for introducing controlled randomization, and showed that speedups of several orders of magnitude could be achieved for state-of-the-art algorithms.

Introducing randomness into algorithms means that a given algorithm run on the same input problem instance has a runtime which follows some initially unknown distribution. There are many reasons why one would want the ability to predict such runtime distributions (RTDs). Luby, Sinclair, and Zuckerman (1993) showed that if one knows the underlying RTD, then it’s possible to construct a fixed cutoff-time restart strategy that is optimal among all possible universal strategies, up to a constant factor. Other popular CSP and SAT solvers use a portfolio of various algorithms, such as SATzilla (Xu et al. 2008) and ArgoSmArT (Nikolić, Marić, and Janičić 2009). Knowing the RTDs of each algorithm in the portfolio allows such solvers to choose the *best* algorithm for a given problem instance.

The majority of the early work for predicting algorithm runtimes involved predicting mean instance runtimes, given the instance’s features. Many of these methods were based on regression variants, such as ridge regression used in SATzilla (Xu et al. 2008).

Gagliolo and Schmidhuber (2005) investigated using a neural network to predict the time remaining before an algorithm reaches the solution on a given problem instance, in the context of algorithm portfolio time allocation. Previous methods for predicting RTDs had separate models for each distribution parameter. DistNet (Eggenesperger, Lindauer, and Hutter 2018) established a new state-of-the-art RTD prediction model which jointly learns the parameters of the RTD by using a neural network. Each output node of the neural network corresponds to a parameter for the given distribution. The neural network’s loss function directly minimizes the negative log-likelihood (NLLH) of the distribution parameters, given the observed runtimes.

Bayesian Neural Networks

Traditional neural networks can be viewed as a probabilistic model: given a dataset $\mathcal{D} = \{(x_i, y_i)\}_{i=1}^N$, the parameterized model $P(\mathbf{y}|\mathbf{x}, \mathbf{w})$ takes in a d -dimensional input $\mathbf{x} \in \mathbb{R}^d$ and computes a point estimate for each output $\mathbf{y} \in \mathcal{Y}$. Training most commonly involves finding the set of weights \mathbf{w} which maximizes the likelihood of the data.

These networks can be prone to overfitting, especially when the number of model parameters is sufficiently greater than the number of training samples. Regularization techniques like using weight priors and dropout (Srivastava et al. 2014) have been proposed to mitigate overfitting.

Bayesian neural networks (BNNs) (MacKay 1992; Neal 2012) extended traditional neural networks by replacing the network’s deterministic weights with a prior distribution over these weights, and using posterior inference. The full posterior distribution of the model’s parameters \mathbf{w} is used when making predictions of unseen data. Prediction for this separate probabilistic model involves taking the expectation over the optimized posterior distribution $P(\mathbf{w}|\mathcal{D})$. The *posterior predictive distribution* of unseen data $(\hat{\mathbf{x}}, \hat{\mathbf{y}})$ is given

by

$$\begin{aligned} P(\hat{\mathbf{y}}|\hat{\mathbf{x}}) &= \mathbb{E}_{P(\mathbf{w}|\mathcal{D})} [P(\hat{\mathbf{y}}|\hat{\mathbf{x}}, \mathbf{w})] \\ &= \int P(\hat{\mathbf{y}}|\hat{\mathbf{x}}, \mathbf{w})P(\mathbf{w}|\mathcal{D}) d\mathbf{w}. \end{aligned}$$

Bayesian neural networks can help with overfitting as the model implicitly involves using an ensemble of an infinite number of neural networks by averaging over all possible weight values, while adding a constant multiple number of network parameters, determined by how many parameters the parametric distribution has. Bayesian neural networks are also able to capture both *aleatoric* uncertainty and *epistemic* uncertainty in its predictions. Aleatoric uncertainty captures uncertainties which are inherent to running statistical trials, like the outcome of a dice toss. This type of uncertainty *cannot* be reduced, no matter how much data is collected. Epistemic uncertainty captures the uncertainty in the model being used, which is due to limited data and/or knowledge. This type of uncertainty *can* be reduced with more data.

Both inference and prediction for BNNs involve calculating the posterior

$$P(\mathbf{w}|\mathcal{D}) = \frac{P(\mathcal{D}|\mathbf{w})P(\mathbf{w})}{P(\mathcal{D})} = \frac{P(\mathcal{D}|\mathbf{w})P(\mathbf{w})}{\int P(\mathcal{D}|\mathbf{w}')P(\mathbf{w}') d\mathbf{w}'}$$

The prior $P(\mathbf{w})$ is something we can choose, but the integral involved in the posterior is often computationally intractable. While the above posterior can be approximated using sampling-based inference algorithms like Markov Chain Monte Carlo (MCMC) methods (Gelfand and Smith 1990), these do not scale well as the number of samples and/or parameters increase (Blei, Kucukelbir, and McAuliffe 2017), as is the case in neural networks. An alternative, suggested by Hinton and Van Camp (1993) and Graves (2011), is to use a variational approximation for the posterior $P(\mathbf{w}|\mathcal{D})$. *Variational methods* construct a new distribution $q(\mathbf{w}|\boldsymbol{\theta})$, parameterized by $\boldsymbol{\theta}$, that approximates the true posterior $P(\mathbf{w}|\mathcal{D})$ by minimizing the Kullback-Leibler (KL) divergence between the two:

$$\begin{aligned} \boldsymbol{\theta}_{\text{VI}} &= \arg \min_{\boldsymbol{\theta}} KL [q(\mathbf{w}|\boldsymbol{\theta}) || P(\mathbf{w}|\mathcal{D})] \\ &= \arg \min_{\boldsymbol{\theta}} \int q(\mathbf{w}|\boldsymbol{\theta}) \log \frac{q(\mathbf{w}|\boldsymbol{\theta})}{P(\mathbf{w})P(\mathcal{D}|\mathbf{w})} d\mathbf{w} \\ &= \arg \min_{\boldsymbol{\theta}} KL [q(\mathbf{w}|\boldsymbol{\theta}) || P(\mathbf{w})] - \mathbb{E}_{q(\mathbf{w}|\boldsymbol{\theta})} [\log P(\mathcal{D}|\mathbf{w})]. \end{aligned}$$

We denote $\boldsymbol{\theta}_{\text{VI}}$ as the parameters found from variational inference methods. Bayes by Backprop (Blundell et al. 2015) uses the above to form the cost function

$$J_{\text{BBB}}(\mathcal{D}, \boldsymbol{\theta}) = KL [q(\mathbf{w}|\boldsymbol{\theta}) || P(\mathbf{w})] - \mathbb{E}_{q(\mathbf{w}|\boldsymbol{\theta})} [\log P(\mathcal{D}|\mathbf{w})]. \quad (1)$$

The intuition for the above cost function is that there is a tradeoff between having a variational posterior that is *close* to the prior we choose yet also able to explain the likelihood of the data. Despite the simple formulation of the above, the cost $J_{\text{BBB}}(\mathcal{D}, \boldsymbol{\theta})$ is still intractable as it involves calculating

posteriors over high-dimensional spaces. While neural networks would seem like an appropriate tool to find a function which minimizes J_{BBB} , we cannot naively apply backpropagation through nodes which involve stochasticity. By applying a generalization of the re-parameterization trick (Oppen and Archambeau 2009; Kingma and Welling 2014), Bayes by Backprop (Blundell et al. 2015) then provides an approximation to the cost (Eq. 1) as

$$J_{\text{BBB}}(\mathcal{D}, \theta) \approx \sum_{i=1}^n \log q(\mathbf{w}^{(i)}|\theta) - \log P(\mathbf{w}^{(i)}) - \log P(\mathcal{D}|\mathbf{w}^{(i)}), \quad (2)$$

where $\mathbf{w}^{(i)}$ is the set of weights drawn from the i -th Monte Carlo sample of the variational posterior $q(\mathbf{w}|\theta)$. Having a computational efficient way of training BNNs has allowed extensions to other network architectures like RNNs (Fortunato, Blundell, and Vinyals 2017) and CNNs (Shridhar, Laumann, and Liwicki 2019), as well as studies into utilizing the uncertainty measures the BNNs provide (Amodei et al. 2016; Kendall and Gal 2017).

3 Problem Formulation

We follow the same problem statement introduced by Eggenperger, Lindauer, and Hutter (2018): A randomized algorithm A is run on a set of n problem instances $\Xi_{\text{train}} = \{\xi_1, \dots, \xi_n\}$. Each instance $\xi \in \Xi_{\text{train}}$ has m instance features $\mathbf{f}(\xi) = [f(\xi)_1, \dots, f(\xi)_m]$. Since algorithm A is randomized, k runtime observations $\mathbf{t}(\xi) = [t(\xi)_1, \dots, t(\xi)_k]$ are gathered by executing A on problem instance ξ , with k different random number generator seeds. The goal is to learn a model that can predict the RTD for unseen instance ξ_{n+1} , given features $\mathbf{f}(\xi_{n+1})$.

Because it is common during the data generation stage to terminate the algorithm on *hard* problem instances which take a long time to solve, the exact runtime may not be known. Ideally, we would like to make use of the measured runtime lower bound without discarding the data and wasting time. From this motivation, we also consider cases where there is censoring, i.e., stopping the algorithm execution if it exceeds a cutoff time t_c . We define the level of censoring as the fraction of runtime observations which are censored due to exceeding a cutoff time t_c . If there are N runtimes in total, with a predetermined level of censoring of c , then t_c is defined as the u -th fastest runtime where $u = \lfloor N(1 - c) \rfloor$. The adjusted runtimes $t'(\xi)_i$ are thus set as $\min(t(\xi)_i, t_c)$ for all i .

4 A Bayesian Approach to Predicting RTDs

Previous methods for predicting RTDs would fit RTD parameters to the set of runtimes for each training instance, then measure loss in the space of RTD parameters β . Eggenperger, Lindauer, and Hutter (2018) introduced DistNet, a new state-of-the-art algorithm runtime prediction model, which is the first of its kind that jointly learns all RTD parameters (as opposed to having independent models for each RTD parameter) by directly minimizing the NLLH loss function.

In this section, we extend DistNet to the Bayesian setting to obtain a more robust model in both low sample settings, and for handling censored observations.

DistNet - A State-of-the-Art Algorithm RTD Prediction Model

Before we introduce our extensions, we give an overview of the DistNet model (Eggenperger, Lindauer, and Hutter 2018). DistNet is a simple feed-forward network for a given distribution \mathcal{F} with distribution parameter vector β . There is one input neuron for each instance feature, and one output neuron for each distribution parameter β_i . The novelty of DistNet is that it directly minimizes the NLLH of the chosen distribution \mathcal{F} . The loss function used in DistNet is

$$J_{\text{DN}}(\mathbf{w}) = - \sum_{\xi \in \Xi_{\text{train}}} \sum_{i=1}^k \log \mathcal{L}_{\mathcal{F}}(\hat{\beta}_{\mathbf{w}, \mathbf{f}(\xi)} | t(\xi)_i), \quad (3)$$

where $\mathcal{L}_{\mathcal{F}}$ is the likelihood function of the parametric distribution \mathcal{F} , and $\hat{\beta}_{\mathbf{w}, \mathbf{f}(\xi)}$ are the parameters of the distribution from the network output, with current weights \mathbf{w} .

Extending DistNet with Bayesian Inference

To extend DistNet with Bayesian inference, which we will refer to as *Bayes DistNet*, a few changes need to be made to the network. We start from the same base network, which has one input neuron for each input feature, and uses simple feed-forward layers.

While the straightforward choice for the Bayesian network output would be the parameters β of the chosen distribution \mathcal{F} , the actual implementation is non-trivial and is computationally expensive. The network would produce a posterior over distribution parameters by sampling the network repeatedly, and these parameters would then be used in the likelihood $\mathcal{L}_{\mathcal{F}}(\hat{\beta}_{\mathbf{w}, \mathbf{f}(\xi)} | t(\xi)_i)$, with the likelihood weighted by the posterior, resulting in a posterior predictive distribution. However, this requires a density estimation method using the set of network samples $\hat{\beta}_{\mathbf{w}, \mathbf{f}(\xi)}$, such that the gradient information can still be tracked from the loss function.

Instead, we choose to have the Bayesian network directly output predicted runtimes \hat{y} . By sampling the network, a sequence of runtimes is produced which is assumed to follow \mathcal{F} . The parameters of \mathcal{F} can then be approximated by computing their maximum likelihood estimates (MLEs), denoted $\hat{\beta}^{\text{MLE}}$. The choice of \mathcal{F} can ensure that we have analytical formulations of $\hat{\beta}^{\text{MLE}}$, which are fast to compute using deep-learning framework intrinsics, and whose gradients can be tracked from the loss function.

To make the network Bayesian, we need to define a variational posterior $q(\mathbf{w}|\theta)$, the prior of the network weights $P(\mathbf{w})$, and the likelihood of the training data. Following Blundell et al. (2015), we assume that the variational posterior $q(\mathbf{w}|\theta)$ is a diagonal Gaussian distribution with mean μ and standard deviation σ . While it is possible to use a multivariate Gaussian, a diagonal Gaussian allows for simple computations without major numerical issues. To be able to use backpropagation, we use the re-parameterization

given by Blundell et al. (2015), which obtains a sample of weights \mathbf{w} for each layer by the following procedure: Sample the parameter-free noise $\epsilon \sim \mathcal{N}(\mathbf{0}, \mathbf{I})$, and let $\sigma = \log(\mathbf{1} + \exp(\rho))$. We can then denote $\theta = (\mu, \rho)$, and the parameterization of σ ensures that the values are always > 0 . The weights \mathbf{w} can then be sampled by $\mathbf{w} = \mu + \sigma \circ \epsilon$, where \circ is point-wise multiplication. Once a particular set of point-wise weights is sampled for each of the layers of the network, those weights are then used as in the traditional feed-forward layers.

Since the network’s task is to predict runtimes directly, it has a single output neuron. The network output \hat{y} represents the predicted runtime for a particular set of point-wise weights which were sampled from each layer. To get a predictive distribution, Monte Carlo sampling is used, in which the same input to the network will be used N times to produce N separate output values.

From Eq. 2, the term $\log P(\mathcal{D}|\mathbf{w})$ is replaced with the likelihood from J_{DN} , which measures the likelihood of the data in our new model. The variational approximated cost function for the network now becomes

$$J(\mathcal{D}, \theta)_{\text{BDN}} = \sum_{i=1}^N \log q(\mathbf{w}^{(i)}|\theta) - \log P(\mathbf{w}^{(i)}) - \sum_{\xi \in \Xi_{\text{train}}} \sum_{j=1}^k \log \mathcal{L}_{\mathcal{F}}(\hat{\beta}^{\text{MLE}}|t(\xi)_j), \quad (4)$$

where $\hat{\beta}^{\text{MLE}}$ is \mathcal{F} ’s distribution parameter vector computed by MLE using the N predicted runtimes \hat{y}_i , and each \hat{y}_i is produced by the network using weights $\mathbf{w}^{(i)}$ from the i -th Monte Carlo sample.

Observing Censored Runtimes

In our application domain, censoring occurs when an algorithm needs to be stopped before completion, i.e., we only know a lower bound on the time it takes to actually complete the algorithm. There is a rich history in survival analysis on handling different types of censored data, and we recommend Klein and Moeschberger (2003) for background reading. Gagliolo and Schmidhuber (2006) first introduced handling *Type I censored sampling* in the context of algorithm runtime prediction, and we give the explanation for clarity.

If censoring time of t_c is used, then t_c is the maximum time an algorithm can run before being terminated. The dataset $\mathcal{D} = \{(\mathbf{f}(\xi)_i, t(\xi)_i)\}_{i=1}^N$ from before now becomes $\mathcal{D} = \{(\mathbf{f}(\xi)_i, t_i, \delta_i)\}_{i=1}^N$, where $t_i = \min(t(\xi)_i, t_c)$, and δ_i is a Boolean variable indicating that an individual sample was not censored (i.e., $\delta_i = 1$ indicates that $t(\xi)_i \leq t_c$).

Let $f_{\mathcal{F}}$ denote the density of distribution \mathcal{F} with parameters β , and let $\mathcal{S}_{\mathcal{F}}$ denote the survival function of distribution \mathcal{F} . If the runtime is not censored, then we observe $\delta_i = 1$, and its contribution to the likelihood function is the density function at that time as it normally would be,

$$\mathcal{L}_{\mathcal{F}}(\hat{\beta}^{\text{MLE}}|t_j) = f_{\mathcal{F}}(t_j|\hat{\beta}^{\text{MLE}}).$$

If the runtime is censored, then we observe $\delta_i = 0$, and all we can say under censoring is that the runtime exceeds the

cutoff t_c . This is equivalent to the survival function, and so its contribution to the likelihood function when censored is

$$\mathcal{L}_{\mathcal{F}}(\hat{\beta}^{\text{MLE}}|t_j) = \mathcal{S}_{\mathcal{F}}(t_j|\hat{\beta}^{\text{MLE}}).$$

Combining the above, we get

$$\mathcal{L}_{\mathcal{F}}(\hat{\beta}^{\text{MLE}}|t_j) = f_{\mathcal{F}}(t_j|\hat{\beta}^{\text{MLE}})^{\delta_j} \mathcal{S}_{\mathcal{F}}(t_j|\hat{\beta}^{\text{MLE}})^{1-\delta_j}, \quad (5)$$

which is then used to replace the likelihood term in the Bayesian cost function (Eq. 4) from above.

Applying Bayes DistNet to RTD Prediction

For comparative results, we follow the same preprocessing steps from Eggenberger, Lindauer, and Hutter (2018). Input instance features are standardized to mean 0 and standard deviation 1, and observed runtimes are scaled into the range of $[0, 1]$. For a level of censoring c , where c is the fraction of censored runtimes from a total of N , the cutoff time t_c is the u -th fastest runtime, where $u = \lfloor N(1 - c) \rfloor$. The runtimes are then set to $\min(t(\xi)_i, t_c)$, and the observations include whether censoring occurred or not.

Both the reference DistNet model and our new Bayesian variant share the majority of the network architecture proposed by Eggenberger, Lindauer, and Hutter. The input layer has a neuron for each instance feature. This is then followed by two hidden fully connected layers, each of which has 16 neurons. DistNet has a fully connected output layer with one neuron per parameter for the specific parametric distribution, whereas Bayes DistNet has a single output.

The Bayes DistNet architecture also has a prior $P(\mathbf{w})$ and a variational posterior $q(\mathbf{w}|\theta)$ that needs to be specified. As previously noted, we use a diagonal Gaussian variational posterior, with initial parameters $\theta_{\text{init}} = (\mu_{\text{init}}, \rho_{\text{init}})$, $\mu_{\text{init}} \sim \mathcal{N}(0, 0.1)$ and $\rho_{\text{init}} \sim \mathcal{N}(-3, 0.1)$. The chosen μ_{init} ensures weights are initialized around 0 (just as we would for a standard neural network), and ρ_{init} is initialized to a small value, as we found learning is not as stable otherwise (Shridhar, Laumann, and Liwicki 2019). For the prior, we follow the proposal from Blundell et al. (2015) of using a mixture of two Gaussian distributions

$$P(\mathbf{w}) = \prod_i \alpha \mathcal{N}(\mathbf{w}_i; 0, \sigma_1^2) + (1 - \alpha) \mathcal{N}(\mathbf{w}_i; 0, \sigma_2^2),$$

where $\mathcal{N}(x; \mu, \sigma^2)$ is the Gaussian density evaluated at x with mean μ and variance σ^2 , with $\alpha = 0.5$, $\sigma_1 = 0.3$, and $\sigma_2 = 0.01$. The choice of these parameters did not have a noticeable difference so long as $\sigma_1 > \sigma_2$ and $\sigma_2 \ll 1$, as per Blundell et al. (2015). When performing inference and prediction, we use 16 Monte Carlo samples. As with previous studies (Fortunato, Blundell, and Vinyals 2017; Shridhar, Laumann, and Liwicki 2019), a large number of samples gives marginally better results at the cost of computation time. We did not find much improvements beyond 16 samples.

DistNet uses the *tanh* activation function, with the exception of the *exponential* activation function on the output layer to ensure the output distribution parameters are > 0 . Bayes DistNet, on the other hand, uses *softplus* (Glorot, Borde, and Bengio 2011) on all layers which is a smooth approximation to the rectifier activation function, as we want

to ensure that activations for variational posterior variances never become ≤ 0 . We then largely follow the hyperparameter choices from Eggenberger, Lindauer, and Hutter (2018), whose DistNet model we are basing our Bayes DistNet model from. Both network architectures use stochastic gradient descent (SGD), with batch normalization (Ioffe and Szegedy 2015), L_2 -regularization of $1e^{-4}$, a learning rate of $1e^{-3}$ which exponentially decays to $1e^{-5}$ over 500 expected epochs, and gradient clipping of $1e^{-2}$. Early stoppage (Prechelt 1998) is used on a separate validation set to reduce overfitting.

5 Experiments

The focus of our experiments is to see how our Bayesian model compares with the current state-of-the-art in low observation number settings, and with various levels of censorship. When gathering data to train the models, using a lower number of observations allows for less time required for the data gathering process. Moreover, being able to handle censored examples also means that one can still use instances which stop prematurely as training data, instead of throwing them away. There are also many domains in which much of the data is censored, such as survival data in medical trials, or nodes that remain in the open list when heuristic search methods are used.

For both experiments, we look at two different algorithms run on different problem instances, with the data gathered by Eggenberger, Lindauer, and Hutter (2018):

- **Clasp-factoring:** The *Clasp* (Gebser, Kaufmann, and Schaub 2012) CDCL solver running on SAT-encoded factorization problems.
- **LPG-Zenotravel:** The *LPG* (Gerevini and Serina 2002) local search solver for planning graphs running on the *Zenotravel* planning domain (Penberthy and Weld 1994).

Both DistNet and Bayes DistNet require a parametric distribution: DistNet directly outputs parameters for this distribution, and both use the distribution in the loss function. For both of the above scenarios, Eggenberger, Lindauer, and Hutter (2018) considered different parametric distributions to use for DistNet. By using the Kolmogorov-Smirnov (KS) goodness-of-fit test, they chose the top two distributions to use in their comparison. For both *Clasp-factoring* and *LPG-Zenotravel*, the inverse Gaussian and lognormal distribution were found to have the closest fit to the empirical distributions as compared to the other considered distributions. In our experiments, we also use these two distributions. The training process uses Python PyTorch 1.5 (Paszke et al. 2019), and we make use of an open source Bayesian Layers PyTorch library (Shridhar, Laumann, and Liwicki 2019). All experiments were run on an Intel i7-7820X and Nvidia GTX 1080 Ti, with 64GB of memory running Ubuntu 16.04.

Low Sample Count per Instance

We evaluated the performance of our Bayes DistNet model by varying the number of observed runtimes per instance. Every instance starts with 100 observed runtimes, and a random subset of those 100 are selected. Having a smaller number of observed runtimes per instance means that the total

training set is reduced. For testing, we keep all 100 observed runtimes for every instance in the test set. The evaluation is performed using a 10-fold cross-validation, repeated with multiple seeds, and aggregating the results.

Figure 1 reports several metrics to evaluate the goodness-of-fit of each model, compared to the empirical observed runtimes of the test set. The likelihood is a way to measure how probable a model is, given the observed data. A lower negative log likelihood (NLLH) thus indicates that one particular model gives the observed data a higher probability of occurring. For both scenarios of *Clasp-factoring* and *LPG-Zenotravel*, Bayes DistNet achieves a lower negative log likelihood across various levels of samples per instance. Given enough data, both DistNet and Bayes DistNet converge to having an equal likelihood score.

While the likelihood is a way to measure how probable a model is given the data, it does not indicate the shape of the predicted runtime distribution. We thus looked at two metrics to quantify how dissimilar the model’s predictive distribution shape is compared to the empirical distribution, namely KL-Divergence and the Kolmogorov-Smirnov statistic (KS-Distance). The KL-Divergence quantifies the amount of information *lost* if the model’s distribution is used instead of the empirical distribution. The KS-Distance measures the maximal distance in height from the model’s CDF to the empirical CDF. For both metrics, lower is better.

Our Bayesian model achieves lower KL-Divergence and lower KS-Distance with respect to the empirical distribution, as compared to the DistNet model across various levels of samples per instance. This indicates that our Bayesian model is able to produce predictive RTDs which are closer in shape to the empirical RTD. Again, given enough data, both DistNet and our Bayesian model converge to predicting RTDs which on average are equally close to the empirical RTDs.

Handling Censored Observations

We also evaluated our Bayes DistNet model by keeping the number of samples per instance constant, but varying the percentage of censoring in the training data. We decided to use 8 samples per instance, as this was the number of samples we start to see both DistNet and our Bayesian variant perform similarly without censoring. To have an accurate comparison, we modified the DistNet loss function to include censored samples as well, following Eq. 5. Figure 2 reports similar metrics as before to evaluate the goodness-of-fit for both DistNet and our Bayesian variant, as compared to the empirical RTDs.

The NLLH of both the best DistNet model and Bayes DistNet are identical under no censoring. As the censoring percentage increases, both models are trained on less fully observable data, and we expect the NLLH to increase. Interestingly, we see that while both models have their NLLH increase, Bayes DistNet increases at a slower rate than DistNet. This indicates that our Bayesian model is better able to capture the uncertainty that comes with using censored data.

Using the distance metrics again, we can see how similar our Bayesian model is to the empirical RTD, as compared to DistNet. We expect both the KL-Divergence and the KS-Distance to increase as the percentage of censored data

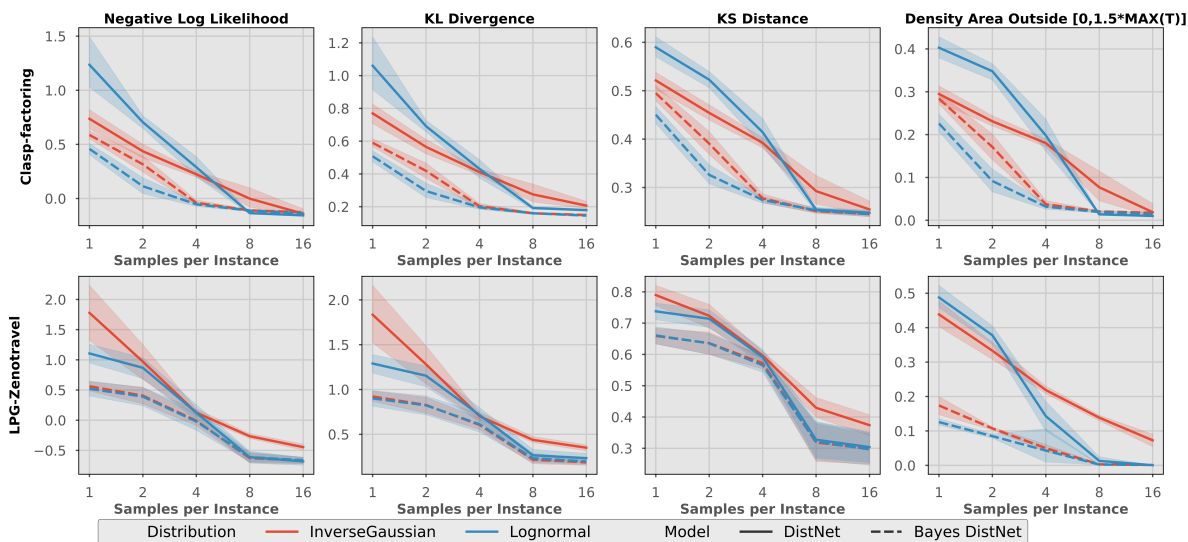


Figure 1: Comparison of DistNet and Bayes DistNet, for various numbers of observed runtimes per instance. Metrics are averaged across 10-folds, repeated for multiple seeds. From left to right: NLLH, KL-Divergence, KS-Distance, and percentage of the density area outside the expected range of 0 to 1.5 times the maximum observed runtime for each instance.

increases. Both the best DistNet model and our Bayesian model start roughly with similar distance metrics. As the percentage of censored data increases, our Bayesian model’s distance metrics increase at a slower rate compared to DistNet. We see that our Bayesian model is able to produce distributions which are more similar to the empirical RTDs under censoring, as compared to DistNet.

Utilizing Model Uncertainty to Recognize Overconfidence

A known issue with standard neural networks, which use point estimates for weights, is that they tend to be overconfident in regions which had little or no data during training. Neural networks fit a function to training data which minimizes the chosen loss function. If deterministic weights are used, then a single particular function of many possible ones is chosen for the data. This function is then extrapolated to make predictions for inputs which may be *far* from the data used to train the network, resulting in overconfident predictions. As a result, adversarial and out-of-distribution inputs can be given to the network, and the network would give predictions which it is confident in, which can be exploited by attackers.

Instead of using point estimates for weights, Bayesian neural networks make predictions using all possible weight values, weighted by their posterior probability. We can think of this as a type of model averaging. When predictions are made for inputs which are far from the data used to train the network, the model averaging considers that there are many possible extrapolations, which result in the confidence regions diverging.

Figure 3 shows the result of traditional neural networks, as is the case for the original DistNet model, of being overconfident in its predictions for adversarial inputs. Both net-

works were trained on the *Clasp-factoring* dataset, except for a held out sample, and both models use the lognormal distribution in the loss function. The held out sample then had all its features shifted by values in the range $[-8, 8]$ to produce a spectrum adversarial samples.

The predictive distribution mean and interquartile ranges were then plotted for these samples. DistNet has small interquartile ranges for adversarial samples, which suggests it does not see adversarial samples any different than the ones it was trained on. This can be problematic if we were to use DistNet in sensitive applications, or scenarios where computation is expensive. On the other hand, Bayes DistNet has interquartile ranges which diverge on adversarial samples. This suggests that Bayes DistNet has the capability to indicate when it is not confident in its predictions. In sensitive or computationally expensive scenarios, a fallback measure can then be used when the predictive distribution’s interquartile range falls outside a given threshold.

Discussion

We have shown that in scenarios featuring a low number of instances or censored observations, our Bayesian model is able to generate distributions which give higher likelihoods of the data, and better match the empirical RTD’s shape.

Both DistNet and Bayes DistNet require a parametric distribution. Both use this distribution in the loss function for the likelihood, but DistNet also restricts the output distribution to directly be a member of that parametric distribution class. From Figures 1 and 2, we can see that the choice of the parametric distribution used has a greater impact on the predictive performance on DistNet, than it does for the Bayesian models. It’s almost certain that RTDs do not perfectly match known parametric distributions. From the data, we can see that putting a restriction on the type of distribu-

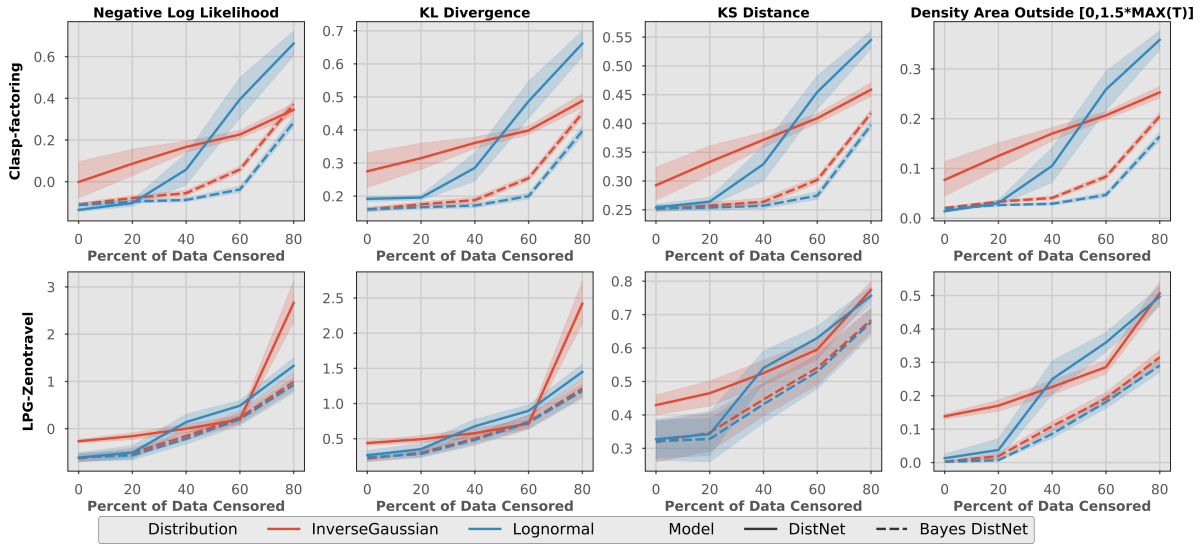


Figure 2: Comparison of DistNet and Bayes DistNet, for various levels of censoring, each with 8 observations per instance. All metrics are averaged across 10-folds, repeated for multiple seeds. From left to right: NLLH, KL-Divergence, KS-Distance, and percentage of density area outside the expected range of 0 to 1.5 times the maximum observed runtime for each instance.

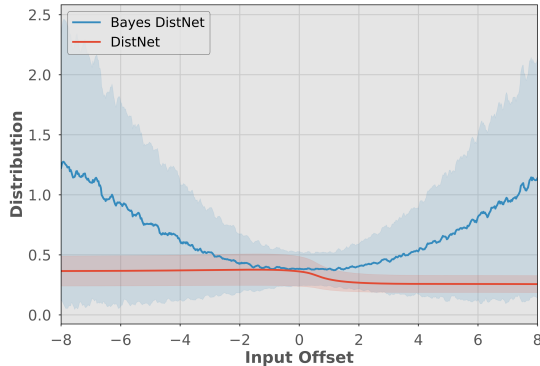


Figure 3: Predictive distributions of adversarial inputs for DistNet and Bayes DistNet. Both models are trained on the *Clasp-factoring* dataset, using the lognormal loss function. Solid lines are mean predictions, with shaded regions showing interquartile ranges.

tions the model can predict can have a negative impact, as is the case for DistNet.

We finally give some insight as to why we believe our Bayesian models outperform DistNet, even when the same parametric distribution is used. For low samples per instance and various levels of censoring, Figures 1 and 2 respectively show where the density of the predicted RTDs lie. We plot the percentage of total area under the RTDs outside the range $[0, T]$, where T is 1.5 times the maximum observed runtime for each instance. We expect that it should be improbable to see many runtimes outside this range, and thus predicted RTDs should give little density outside this range if the density is to be informative. When a low number of samples is used, we can see from Figure 1 that in some cases, DistNet

is unable to give an informative predictive RTD, as a significant amount of density is outside the predictable range. For the censored cases, Figure 2 shows similar results.

We summarize in that both DistNet and our Bayesian variant perform similarly if given enough non-censored data. As the level of censoring increases and as the number of samples per instance decreases, our Bayesian model starts to outperform DistNet and better matches the empirical RTDs. It appears from our results that the discrepancy in performance between the Bayesian and non-Bayesian versions is more affected by the number of samples used.

6 Conclusions and Future Work

In this paper, we have shown that the existing state-of-the-art RTD prediction model can be extended to the Bayesian setting. Our Bayesian model Bayes DistNet outperforms the previous state-of-the-art in the low observation setting, as well as with handling censored examples. The Bayesian model also lifts some of the restrictions that occur when previous models could only output an explicit parametric distribution, when many randomized algorithms do not perfectly follow these parametric distributions.

Both DistNet and Bayes DistNet require a parametric distribution \mathcal{F} to quantify the likelihood in the loss function. As previously mentioned, we chose for our Bayesian network to output predicted runtimes directly instead of \mathcal{F} 's parameters. We see as future work coming up with an efficient method to have the network output \mathcal{F} 's parameters, and compare it with our method. We would also like to see further extensions of this work which do not depend on a restrictive class of parametric distributions. Finally, existing algorithm portfolio methods can be extended to utilize the features of our Bayesian network, such as having access to the uncertainty in predicting runtime distributions.

References

- Amodei, D.; Olah, C.; Steinhardt, J.; Christiano, P.; Schulman, J.; and Mané, D. 2016. Concrete problems in AI safety.
- Blei, D. M.; Kucukelbir, A.; and McAuliffe, J. D. 2017. Variational inference: A review for statisticians. *Journal of the American statistical Association* 112(518): 859–877.
- Blundell, C.; Cornebise, J.; Kavukcuoglu, K.; and Wierstra, D. 2015. Weight uncertainty in neural network. In Bach, F.; and Blei, D., eds., *Proceedings of the 32nd International Conference on Machine Learning*, volume 37 of *Proceedings of Machine Learning Research*, 1613–1622. Lille, France: PMLR. URL <http://proceedings.mlr.press/v37/blundell15.html>.
- Eggensperger, K.; Lindauer, M.; and Hutter, F. 2018. Neural networks for predicting algorithm runtime distributions. In *Proceedings of the Twenty-Seventh International Joint Conference on Artificial Intelligence, IJCAI-18*, 1442–1448. International Joint Conferences on Artificial Intelligence Organization. doi:10.24963/ijcai.2018/200. URL <https://doi.org/10.24963/ijcai.2018/200>.
- Fortunato, M.; Blundell, C.; and Vinyals, O. 2017. Bayesian recurrent neural networks.
- Gagliolo, M.; and Schmidhuber, J. 2005. A neural network model for inter-problem adaptive online time allocation. In *International Conference on Artificial Neural Networks*, 7–12. Springer.
- Gagliolo, M.; and Schmidhuber, J. 2006. Impact of censored sampling on the performance of restart strategies. *Lecture Notes in Computer Science (including subseries Lecture Notes in Artificial Intelligence and Lecture Notes in Bioinformatics)* 4204 LNCS: 167–181. ISSN 16113349. doi:10.1007/11889205_14.
- Gebser, M.; Kaufmann, B.; and Schaub, T. 2012. Conflict-driven answer set solving: From theory to practice. *Artif. Intell.* 187–188: 52–89. ISSN 0004-3702. doi:10.1016/j.artint.2012.04.001.
- Gelfand, A. E.; and Smith, A. F. 1990. Sampling-based approaches to calculating marginal densities. *Journal of the American statistical association* 85(410): 398–409.
- Gerevini, A.; and Serina, I. 2002. LPG: A planner based on local search for planning graphs with action costs. In *Proceedings of the Sixth International Conference on Artificial Intelligence Planning Systems, AIPS'02*, 13–22. AAAI Press. ISBN 1577351428.
- Glorot, X.; Bordes, A.; and Bengio, Y. 2011. Deep sparse rectifier neural networks. In *Proceedings of the fourteenth international conference on artificial intelligence and statistics*, 315–323.
- Gomes, C. P.; Selman, B.; and Kautz, H. 1998. Boosting combinatorial search through randomization. In *Proceedings of the Fifteenth National/Tenth Conference on Artificial Intelligence/Innovative Applications of Artificial Intelligence, AAAI '98/IAAI '98*, 431–437. USA: American Association for Artificial Intelligence. ISBN 0262510987.
- Graves, A. 2011. Practical variational inference for neural networks. In *Advances in neural information processing systems*, 2348–2356.
- Harvey, W. D. 1995. *Nonsystematic backtracking search*. Ph.D. thesis, Stanford, CA, USA.
- Hinton, G. E.; and Van Camp, D. 1993. Keeping the neural networks simple by minimizing the description length of the weights. In *Proceedings of the sixth annual conference on Computational learning theory*, 5–13.
- Ioffe, S.; and Szegedy, C. 2015. Batch normalization: Accelerating deep network training by reducing internal covariate shift.
- Kendall, A.; and Gal, Y. 2017. What uncertainties do we need in Bayesian deep learning for computer vision? In *Advances in neural information processing systems*, 5574–5584.
- Kingma, D. P.; and Welling, M. 2014. Auto-Encoding Variational Bayes. *CoRR* abs/1312.6114.
- Klein, J. P.; and Moeschberger, M. L. 2003. *Survival analysis techniques for censored and truncated data*. Second edition.
- Luby, M.; Sinclair, A.; and Zuckerman, D. 1993. Optimal speedup of Las Vegas algorithms. *Information Processing Letters* 47(4): 173–180. ISSN 00200190. doi:10.1016/0020-0190(93)90029-9.
- MacKay, D. J. 1992. A practical Bayesian framework for backpropagation networks. *Neural computation* 4(3): 448–472.
- Neal, R. M. 2012. *Bayesian learning for neural networks*, volume 118. Springer Science & Business Media.
- Nikolić, M.; Marić, F.; and Janičić, P. 2009. Instance-based selection of policies for SAT solvers. In Kullmann, O., ed., *Theory and Applications of Satisfiability Testing - SAT 2009*, 326–340. Berlin, Heidelberg: Springer Berlin Heidelberg. ISBN 978-3-642-02777-2.
- Opper, M.; and Archambeau, C. 2009. The variational Gaussian approximation revisited. *Neural computation* 21(3): 786–792.
- Paszke, A.; Gross, S.; Massa, F.; Lerer, A.; Bradbury, J.; Chanan, G.; Killeen, T.; Lin, Z.; Gimelshein, N.; Antiga, L.; Desmaison, A.; Kopf, A.; Yang, E.; DeVito, Z.; Raison, M.; Tejani, A.; Chilamkurthy, S.; Steiner, B.; Fang, L.; Bai, J.; and Chintala, S. 2019. PyTorch: An imperative style, high-performance deep learning library. In *Advances in Neural Information Processing Systems* 32, 8024–8035. Curran Associates, Inc. URL <http://papers.neurips.cc/paper/9015-pytorch-an-imperative-style-high-performance-deep-learning-library.pdf>.
- Penberthy, J. S.; and Weld, D. S. 1994. Temporal planning with continuous change. In *Proceedings of the Twelfth AAAI National Conference on Artificial Intelligence, AAAI'94*, 1010–1015. AAAI Press.
- Prechelt, L. 1998. Automatic early stopping using cross validation: quantifying the criteria. *Neural Networks* 11(4): 761–767.

Shridhar, K.; Laumann, F.; and Liwicki, M. 2019. A comprehensive guide to Bayesian convolutional neural network with variational inference.

Srivastava, N.; Hinton, G.; Krizhevsky, A.; Sutskever, I.; and Salakhutdinov, R. 2014. Dropout: a simple way to prevent neural networks from overfitting. *The journal of machine learning research* 15(1): 1929–1958.

Xu, L.; Hutter, F.; Hoos, H. H.; and Leyton-Brown, K. 2008. SATzilla: portfolio-based algorithm selection for SAT. *Journal of artificial intelligence research* 32: 565–606.

Appendix

Scenario	Num Samples	Model	Distribution	NLLH	KLD	D-KS	Mass
clasp_factoring	1	Bayes DistNet	InverseGaussian	0.587 ± 0.089	0.590 ± 0.060	0.495 ± 0.035	0.284 ± 0.030
			Lognormal	0.459 ± 0.123	0.508 ± 0.081	0.450 ± 0.043	0.226 ± 0.047
		DistNet	InverseGaussian	0.737 ± 0.205	0.770 ± 0.139	0.521 ± 0.042	0.295 ± 0.044
			Lognormal	1.236 ± 0.557	1.061 ± 0.383	0.590 ± 0.051	0.403 ± 0.058
clasp_factoring	2	Bayes DistNet	InverseGaussian	0.316 ± 0.180	0.419 ± 0.115	0.391 ± 0.057	0.171 ± 0.073
			Lognormal	0.113 ± 0.165	0.295 ± 0.103	0.326 ± 0.050	0.092 ± 0.062
		DistNet	InverseGaussian	0.436 ± 0.152	0.565 ± 0.106	0.454 ± 0.038	0.231 ± 0.029
			Lognormal	0.705 ± 0.137	0.691 ± 0.090	0.523 ± 0.041	0.348 ± 0.044
clasp_factoring	4	Bayes DistNet	InverseGaussian	-0.040 ± 0.060	0.203 ± 0.037	0.277 ± 0.021	0.037 ± 0.018
			Lognormal	-0.054 ± 0.051	0.196 ± 0.032	0.274 ± 0.015	0.032 ± 0.015
		DistNet	InverseGaussian	0.224 ± 0.065	0.412 ± 0.044	0.392 ± 0.026	0.180 ± 0.022
			Lognormal	0.289 ± 0.213	0.431 ± 0.133	0.414 ± 0.069	0.198 ± 0.086
clasp_factoring	8	Bayes DistNet	InverseGaussian	-0.110 ± 0.021	0.160 ± 0.016	0.251 ± 0.012	0.021 ± 0.004
			Lognormal	-0.112 ± 0.025	0.160 ± 0.017	0.253 ± 0.012	0.019 ± 0.006
		DistNet	InverseGaussian	-0.001 ± 0.202	0.275 ± 0.130	0.293 ± 0.069	0.077 ± 0.084
			Lognormal	-0.135 ± 0.022	0.192 ± 0.018	0.254 ± 0.012	0.014 ± 0.003
clasp_factoring	16	Bayes DistNet	InverseGaussian	-0.127 ± 0.023	0.149 ± 0.016	0.245 ± 0.014	0.018 ± 0.004
			Lognormal	-0.136 ± 0.022	0.145 ± 0.015	0.245 ± 0.012	0.014 ± 0.004
		DistNet	InverseGaussian	-0.140 ± 0.096	0.207 ± 0.054	0.255 ± 0.035	0.019 ± 0.044
			Lognormal	-0.156 ± 0.022	0.179 ± 0.018	0.248 ± 0.013	0.010 ± 0.002
lpg-zeno	1	Bayes DistNet	InverseGaussian	0.562 ± 0.167	0.923 ± 0.126	0.659 ± 0.060	0.174 ± 0.065
			Lognormal	0.520 ± 0.292	0.901 ± 0.208	0.661 ± 0.066	0.126 ± 0.023
		DistNet	InverseGaussian	1.779 ± 1.106	1.835 ± 0.762	0.790 ± 0.073	0.438 ± 0.087
			Lognormal	1.106 ± 0.368	1.290 ± 0.253	0.738 ± 0.065	0.488 ± 0.078
lpg-zeno	2	Bayes DistNet	InverseGaussian	0.407 ± 0.316	0.827 ± 0.220	0.636 ± 0.079	0.107 ± 0.010
			Lognormal	0.391 ± 0.369	0.823 ± 0.253	0.635 ± 0.082	0.085 ± 0.014
		DistNet	InverseGaussian	0.970 ± 0.700	1.281 ± 0.498	0.723 ± 0.088	0.333 ± 0.058
			Lognormal	0.868 ± 0.403	1.154 ± 0.276	0.714 ± 0.070	0.378 ± 0.060
lpg-zeno	4	Bayes DistNet	InverseGaussian	-0.009 ± 0.234	0.605 ± 0.150	0.572 ± 0.049	0.050 ± 0.026
			Lognormal	-0.021 ± 0.422	0.612 ± 0.257	0.565 ± 0.060	0.043 ± 0.135
		DistNet	InverseGaussian	0.126 ± 0.136	0.702 ± 0.101	0.596 ± 0.035	0.219 ± 0.026
			Lognormal	0.126 ± 0.303	0.716 ± 0.193	0.591 ± 0.057	0.143 ± 0.106
lpg-zeno	8	Bayes DistNet	InverseGaussian	-0.627 ± 0.183	0.217 ± 0.118	0.319 ± 0.139	0.003 ± 0.002
			Lognormal	-0.611 ± 0.192	0.232 ± 0.124	0.321 ± 0.145	0.002 ± 0.002
		DistNet	InverseGaussian	-0.265 ± 0.093	0.438 ± 0.079	0.429 ± 0.074	0.139 ± 0.019
			Lognormal	-0.613 ± 0.239	0.266 ± 0.159	0.327 ± 0.137	0.013 ± 0.027
lpg-zeno	16	Bayes DistNet	InverseGaussian	-0.672 ± 0.119	0.186 ± 0.075	0.298 ± 0.117	0.001 ± 0.001
			Lognormal	-0.664 ± 0.127	0.197 ± 0.080	0.297 ± 0.124	0.001 ± 0.001
		DistNet	InverseGaussian	-0.446 ± 0.120	0.350 ± 0.084	0.374 ± 0.079	0.073 ± 0.043
			Lognormal	-0.682 ± 0.160	0.234 ± 0.120	0.304 ± 0.119	0.000 ± 0.000

Table 1: Table corresponding to Figure 1. Comparison of DistNet and Bayes DistNet, for various numbers of observed runtimes per instance. Metrics are averaged across 10-folds, repeated for multiple seeds. From left to right: NLLH, KL-Divergence, KS-Distance, and percentage of density area outside the expected range of 0 to 1.5 times the maximum observed runtime for each instance.

Scenario	Lower Bound	Model	Distribution	NLLH	KLD	D-KS	Mass
clasp_factoring	0	Bayes DistNet	InverseGaussian	-0.110 ± 0.021	0.160 ± 0.016	0.251 ± 0.012	0.021 ± 0.004
			Lognormal	-0.112 ± 0.025	0.160 ± 0.017	0.253 ± 0.012	0.019 ± 0.006
		DistNet	InverseGaussian	-0.001 ± 0.202	0.275 ± 0.130	0.293 ± 0.069	0.077 ± 0.084
			Lognormal	-0.135 ± 0.022	0.192 ± 0.018	0.254 ± 0.012	0.014 ± 0.003
clasp_factoring	20	Bayes DistNet	InverseGaussian	-0.078 ± 0.025	0.175 ± 0.017	0.257 ± 0.012	0.033 ± 0.006
			Lognormal	-0.095 ± 0.022	0.166 ± 0.016	0.254 ± 0.012	0.026 ± 0.005
		DistNet	InverseGaussian	0.087 ± 0.150	0.315 ± 0.099	0.333 ± 0.058	0.125 ± 0.064
			Lognormal	-0.103 ± 0.036	0.196 ± 0.020	0.264 ± 0.017	0.031 ± 0.015
clasp_factoring	40	Bayes DistNet	InverseGaussian	-0.055 ± 0.033	0.188 ± 0.021	0.264 ± 0.016	0.041 ± 0.010
			Lognormal	-0.087 ± 0.025	0.172 ± 0.017	0.257 ± 0.012	0.029 ± 0.007
		DistNet	InverseGaussian	0.167 ± 0.065	0.361 ± 0.040	0.372 ± 0.031	0.170 ± 0.031
			Lognormal	0.058 ± 0.179	0.285 ± 0.102	0.329 ± 0.072	0.105 ± 0.086
clasp_factoring	60	Bayes DistNet	InverseGaussian	0.059 ± 0.037	0.254 ± 0.022	0.302 ± 0.014	0.084 ± 0.014
			Lognormal	-0.037 ± 0.037	0.200 ± 0.022	0.275 ± 0.016	0.047 ± 0.013
		DistNet	InverseGaussian	0.227 ± 0.045	0.399 ± 0.030	0.409 ± 0.019	0.207 ± 0.019
			Lognormal	0.395 ± 0.221	0.487 ± 0.134	0.455 ± 0.072	0.259 ± 0.091
clasp_factoring	80	Bayes DistNet	InverseGaussian	0.372 ± 0.050	0.451 ± 0.033	0.418 ± 0.014	0.205 ± 0.020
			Lognormal	0.285 ± 0.057	0.397 ± 0.036	0.397 ± 0.018	0.164 ± 0.021
		DistNet	InverseGaussian	0.345 ± 0.072	0.488 ± 0.051	0.459 ± 0.029	0.253 ± 0.028
			Lognormal	0.663 ± 0.138	0.661 ± 0.090	0.545 ± 0.038	0.358 ± 0.045
lpg-zeno	0	Bayes DistNet	InverseGaussian	-0.627 ± 0.183	0.217 ± 0.118	0.319 ± 0.139	0.003 ± 0.002
			Lognormal	-0.611 ± 0.192	0.232 ± 0.124	0.321 ± 0.145	0.002 ± 0.002
		DistNet	InverseGaussian	-0.265 ± 0.093	0.438 ± 0.079	0.429 ± 0.074	0.139 ± 0.019
			Lognormal	-0.613 ± 0.239	0.266 ± 0.159	0.327 ± 0.137	0.013 ± 0.027
lpg-zeno	20	Bayes DistNet	InverseGaussian	-0.509 ± 0.217	0.300 ± 0.141	0.347 ± 0.135	0.019 ± 0.020
			Lognormal	-0.561 ± 0.226	0.284 ± 0.138	0.328 ± 0.153	0.007 ± 0.009
		DistNet	InverseGaussian	-0.158 ± 0.175	0.493 ± 0.122	0.465 ± 0.093	0.170 ± 0.041
			Lognormal	-0.505 ± 0.338	0.352 ± 0.186	0.343 ± 0.162	0.038 ± 0.074
lpg-zeno	40	Bayes DistNet	InverseGaussian	-0.155 ± 0.235	0.501 ± 0.158	0.446 ± 0.121	0.109 ± 0.033
			Lognormal	-0.214 ± 0.281	0.483 ± 0.184	0.432 ± 0.134	0.086 ± 0.032
		DistNet	InverseGaussian	-0.000 ± 0.226	0.579 ± 0.155	0.525 ± 0.089	0.226 ± 0.053
			Lognormal	0.139 ± 0.393	0.677 ± 0.244	0.540 ± 0.118	0.250 ± 0.117
lpg-zeno	60	Bayes DistNet	InverseGaussian	0.234 ± 0.311	0.740 ± 0.207	0.541 ± 0.119	0.192 ± 0.042
			Lognormal	0.201 ± 0.341	0.729 ± 0.225	0.529 ± 0.126	0.181 ± 0.045
		DistNet	InverseGaussian	0.194 ± 0.204	0.714 ± 0.141	0.596 ± 0.073	0.286 ± 0.046
			Lognormal	0.487 ± 0.287	0.897 ± 0.186	0.630 ± 0.084	0.359 ± 0.068
lpg-zeno	80	Bayes DistNet	InverseGaussian	0.993 ± 0.421	1.214 ± 0.277	0.684 ± 0.088	0.315 ± 0.054
			Lognormal	0.926 ± 0.391	1.179 ± 0.259	0.677 ± 0.092	0.290 ± 0.049
		DistNet	InverseGaussian	2.663 ± 1.033	2.419 ± 0.698	0.774 ± 0.060	0.507 ± 0.081
			Lognormal	1.330 ± 0.394	1.449 ± 0.260	0.757 ± 0.066	0.497 ± 0.074

Table 2: Table corresponding to Figure 2. Comparison of DistNet and Bayes DistNet, for various levels of censoring, each with 8 observations per instance. Metrics are averaged across 10-folds, repeated for multiple seeds. From left to right: NLLH, KL-Divergence, KS-Distance, and percentage of density area outside the expected range of 0 to 1.5 times the maximum observed runtime for each instance.